Production and Growth of New Particles during Two Cruise Campaigns in the Marginal Seas of China

Xiaohuan Liu[1], Yujiao Zhu[1], Mei Zheng[2#], Huiwang Gao[1], Xiaohong Yao[1,3#]

[1] Key Laboratory of Marine Environment and Ecology, Ministry of Education of China, Ocean University of China, Qingdao 266100, China

[2] State Key Joint Laboratory for Environmental Simulation and Pollution Control, College of Environmental Sciences and Engineering, Peking University, Beijing 100871, China

[3]Qingdao Collaborative Center of Marine Science and Technology, Qingdao 266100, China

Corresponding authors: xhyao@ouc.edu.cn, mzheng@pku.edu.cn

Abstract

In this paper, we investigated production and growth of new particles in the marine atmosphere during two cruise campaigns in China Seas using a Fast Mobility Particle Sizer. Only eight new particle formation (NPF) events (> 30 min) occurred on 5 days out of 31 sampling days and the subsequent growth of new particles were observed only in five events. Apparent formation rates of new particles (in the range of 5.6-30 nm) varied from 0.3 to 15.2 particles cm^{-3} s^{-1} in eight events and growth rates ranged from 2.5 to 10 nm h^{-1} in five NPF events. Modeling results simulated by U.S. EPA Community Multi-scale Air Quality Model (CMAQ) showed that ammonium nitrate (NH_4NO_3) was newly formed in the atmosphere over the corresponding sea zone

during 2 out of 5 events, in which new particles partially or mostly grew over 50 nm. However, in the remaining three events, new particles cannot grow over 30 nm and the modeling results showed that no NH_4NO_3 was newly formed in the corresponding marine atmosphere. Modeling results also showed that formation of secondary organics occurred through all new particle growth periods. Difference between the two types of new particle growth patterns suggested that a combination of ammonium nitrate and organics newly formed likely contributed to the growth of new particles from 30 nm to larger size. However, the findings were obtained from the limited data and the simulations of CMAQ also suffered from several weaknesses such as only having three size bins for different particles, lack of marine aerosol precursors, etc. More future study is thereby needed for confirmation.

Keywords: new particle formation, ammonium nitrate, secondary organics, China Seas, CMAQ model

1. Introduction

Atmospheric particles play important roles in regional visibility deterioration and global climate change by directly scattering and absorbing the sunlight and indirectly acting as cloud condensation nuclei (CCN) (Sloane et al., 1991; Curtius, 2006; IPCC, 2007; Luo and Yu, 2011) and they have primary and secondary origins (Holmes, 2007; Kulmala and Kerminen, 2008; Pierce et al., 2012; Riipinen et al., 2011, 2012; Yao and Zhang, 2011). Nucleation has been reported as an important secondary source of atmospheric particles because it can quickly increase the number concentration of

atmospheric particles from hundreds to dozens of thousands particles per cubic centimeter air in a few hours (Kulmala and Kerminen, 2008). However, atmospheric particles <30 nm in diameter are conventionally considered to be nucleation mode particles and particles in this size range are less likely to be activated as CCN under the typical range of atmospheric supersaturation (Dall'Osto et al., 2005; Dusek et al., 2006; Quinn et al., 2008). New particles growing over 50 nm in diameter have been found to be an important source of CCN while ~80 nm particles can be activated to be CCN at a moderate supersaturation (e.g., ~0.2%, Petters and Kreidenweis, 2007; Pierce and Adams, 2009; Pierce et al., 2012; Riipinen et al., 2011, 2012). The size of new particles can be used to roughly evaluate their potential as CCN, although other factors such as their chemical composition and mixing state also affect the potential (Dusek et al., 2006; Quinn et al., 2008; Kerminen et al., 2012). However, it is still quite unclear which chemicals contribute to the condensational growth of new particles to CCN size (Kulmala et al., 2013), particularly the growth of new particles from ~ 30 nm to CCN size.

Oceans account for approximately 70% of areas on the earth. Huge efforts have been taken to improve understanding of the relationship between production of new particles in marine atmosphere and their impacts on the climate in the last three decades (Charlson et al., 1987; O'Dowd et al., 2007; Quinn and Bates, 2011). Several earlier studies focused on new particle formation (NPF) in remote marine atmosphere and some clear coastal environments such as Mace Head, where dimethylsulfide (DMS) and iodine have been proposed to be important precursors for new particles

(Cover et al., 1996; Clarke et al, 1998; O'Dowd et al., 2002; O'Dowd et al., 2007; Chang et al., 2011). In polluted marine atmosphere, high concentrations of secondary particulate species generated from anthropogenic and/or biogenic precursors as well as a small amount of particulate methanesulfonic acid from marine biogenic sources were frequently observed and these observed species were proposed to have important impacts on regional climate (Yang et al., 2009; Shi et al., 2010; Feng et al., 2012; Wang et al., 2014). For indirect climate effects, the number concentration of atmospheric particles is critical. However, direct measurements of NPF events are still limited and the same can be said for assessing their potential contribution to CCN (Lin et al., 2007). In addition, the characters of NPF among in polluted, remote marine and clear coastal environments could be very different. Thus, more observations for NPF events in polluted marine atmosphere are essential.

To improve understanding the characters of NPF events in polluted marine atmosphere in different extents and evaluating their potential climatic impacts, we investigated NPF and their subsequent growth in the marginal seas of China including the Yellow Sea and the East China Sea during two cruise campaigns from 16 October to 5 November 2011 and from 2 to 11 November 2012. A Fast Mobility Particle Sizer spectrometer (FMPS) was used for on-board sampling to study NPF events and the US EPA Community Multi-scale Air Quality Model (CMAQ) was used to simulate chemical and physical processes of particulate species over the study marginal seas to facilitate data analysis. On five days during the two campaigns, eight NPF events with or without a subsequent growth of new particles were observed. An in-depth analysis

was conducted to interpret these events with a particular attention to investigate factors determining the growth of 30-40 nm new particles to larger size.

2. Experimental

2.1 Cruise routes, particle sizers and computer method

In the fall of 2011 and 2012, two cruise campaigns were organized by Ocean University of China (OUC) using a research vessel *Dongfanghong* 2 (Fig. 1a and b). The two campaigns were to provide services for research projects funded by National Natural Science Foundation of China and these projects covered a variety of basic research from sea bed to lower layer marine atmosphere. The cruise route during the period 16 October to 5 November 2011 included the south Yellow Sea and the East China Sea, while the second campaign was limited in the south Yellow Sea during the period of 2-11 November 2012.

A FMPS (TSI Model 3091) downstream of a dryer (TSI, 3091) was used for measuring number concentrations of marine atmospheric particles in one-second time resolution, which was placed on the front board of *Dongfanghong* 2. To investigate the potential relationship of NPF events between in-land and marine atmosphere, simultaneous measurements were conducted at a 5-story building in the campus of Ocean University of China (Lat:36.1°N, Long:120.5°E, distance to the nearest coast line is 7.5 km) using a NanoScan Scanning Mobility Particle Sizer Spectrometer (SMPS) Nanoparticle Sizer (TSI, 3910) in Novermber 2012, but not in November 2011. The sizer was equipped with a Radial Differential Mobility Analyzer (RDMA) and an internal Condensation Particle Counter (CPC) and operated in one-minute time

resolution. Particle apparent formation rate (J_{30}) was calculated using the method provided by Dal Maso et al. (2005):

$$J_{30} = dN_{<30nm} / dt + F_{growth} + F_{coag} \quad (1)$$

where $N_{<30nm}$ is the number concentrations of the 5.6-30 nm particles for the FMPS and 10-30 nm for the NanoScan SMPS during the initial 1-2 h of new particle burst; F_{growth} (the flux of particles grow out of the size range, we chose the size range for the nucleated particles to be 5.6-30 nm) is conventionally assumed to be zero, because particles rarely grew out of 30 nm in the initial 1-2 h (Dal Maso et al., 2005); F_{coag} is the sum of particle-particle inter- and hetero-coagulation rate calculated in the same way as Yao et al. (2005).

Particles size distributions in this study were not uni-modal during most of the time, and they were dominated by bi-modal distribution. Therefore, aerosol particle size distributions in this study are fitted with the multi log-normal distribution function (Whitby, 1978), which is expressed mathematically by:

$$f(D_p, D_{pg,i}, C_i, \sigma_{g,i}) = \sum_{i=1}^{n} \frac{C_i}{(2\pi)^{1/2} \log(\sigma_{g,i})} \times \exp[-\frac{[\log(D_p) - \log(D_{pg,i})]^2}{2\log^2(\sigma_{g,i})}] \quad (2)$$

where D_p is the diameter of aerosol particle. Three parameters characterize an individual log-normal mode *i*: the mode number concentration C_i, geometric variance $\sigma_{g,i}^2$, and geometric mean diameter $D_{pg,i}$. The number of individual log-normal modes that characterize the particle number size distribution is denoted by *n* (*i* is in the range of 1-*n*). In this study, *n* is usually equal to 2, and $D_{pg,1}$ represents for the geometric median diameter of new particles followed by particle growth in the observed events. The growth of preexisting Aitken mode particles was also observed in this study, and $D_{pg,2}$ represents for the geometric median diameter of the preexisting

particles.

Particle apparent growth rate (GR) in this study was calculated by:

$$GR = \frac{\Delta D_{pg,i}}{\Delta t} \quad (3)$$

where Δt is the time slot for the growth of particles. Particle apparent shrinkage rate (SR) was calculated using the same equation as GR but the value is negative.

2.2 Model description

The U.S. EPA Community Multi-scale Air Quality Model (CMAQ v4.7.1; Byun and Ching, 1999) was used for simulating concentrations of gases and particulate species in $PM_{2.5}$ during NPF events. The meteorological data were provided by the Weather Research and Forecasting (WRF) model (v3.2) (Skamarock et al., 2008) and processed by the Meteorological-Chemical Interface Processor (MCIP v3.3) for CMAQ-ready inputs. Emissions were generated on basis of the NASA's project emission inventory (The Intercontinental Chemical Transport Experiment Phase B, INTEX-B, Q. Zhang et al., 2009; Liu et al., 2010a), which included major air pollutants such as SO_2, NO_x, CO, and 30 lumped VOC species. The vertical resolution includes 14 logarithmic structure layers from the surface to the tropopause, with the first model layer height of 36 m above the ground level, while the horizontal resolution is 36 × 36 km. Particle in CMAQ is represented by three lognormal sub-distributions, e.g., Aitken, accumulation and coarse mode. Riipinen et al (2011) and Ehn et al (2014) recently reported the important role of extremely low volatility secondary organic aerosol (SOA) in growing <30 nm new particles in continental atmosphere. In CMAQ version4.7.1, four types of non-volatile SOA were simulated**,**

while other SOA species was treated as semi-volatile (Carlton et al., 2010). Validation of CMAQ application in China has been reported by Liu et al. (2010a, b). The CMAQ model does not include chemical reactions of amines which have been proposed as an important species to grow nucleated particles (Smith and Mueller, 2010; Riipinen et al., 2012; Zhang et al., 2012; Kulmala et al., 2013). Thus, contributions of amines to new particle growth will not be discussed in this study.

2.3 On-site meteorological data and satellite data

Wind speed, wind direction, relatively humidity, air temperature and solar radiation were measured continuously on board and synchronously. Daily averaged sea surface chlorophyll a concentrations were derived from Standard Mapped Image products observed by Moderate Resolution Imaging Spectroradiometer (MODIS)/AQUA SMI products. Horizontal resolution is 4 × 4 km (Tan et al., 2011).

3. Results

NPF events (>30 min) were observed on four days during the cruise campaign in 2011. However, there was only one day when NPF events were observed in the cruise campaign in 2012 (Fig. S1a and b). On the same day, a NPF event was also observed at the site of OUC. All these NPF events in the marine atmosphere started to be observed at the locations, which are 30-120 km away from the nearest coastline (Fig. 1a and b, Table 1). In these events, the total number concentration of <30 nm particles increased from ~0.5×10^3 particles cm^{-3} to ~2.5×10^4 particles cm^{-3} within 0.5~4 h. We will first examine the production and growth processes of the events in 2012 in Sect.

3.1, while in Sects. 3.2 and 3.3, events in 2011 will be studied.

3.1 NPF events in the fall cruise campaign of 2012

In November 2012, two particle sizers were used for measurements on board and on the land, respectively. The observation can allow an investigation of regional characteristics of NPF events. A heavy rain event occurred at the night on 3 November 2012 with wind speed of 10-14 m s^{-1}. The rainfall and the strong wind substantially removed preexisting atmospheric particles and NPF events were observed both in the marine and coastal atmosphere in the daytime of 4 November (Day 1, Fig. 2). On Day 1, *Dongfanghong 2* was anchored at approximately 80 km distance southeast of OUC and the location was about 60 km away from the nearest coastline (Fig. 1b).

3.1.1 Formation rates of new particles

Two NPF events were observed on Day 1 in the marine atmosphere. The first one was observed since 07:50LT and reached the maximum at 08:43LT (Fig. 2a and b). The initial size of new particles was ~6 nm which is the detection limit of FMPS. The nucleation mode particles (<30 nm) increased from $<1.0\times10^3$ particles cm^{-3} before 07:50 to 1.0×10^4 particles cm^{-3} at 08:43LT and the apparent formation rate of new particles was calculated to be 1.4 particles $cm^{-3}s^{-1}$. No particle growth was observed before 08:43LT. The second NPF event was observed after 09:24LT. Nucleation mode particles increased from 0.4×10^4 to 2.5×10^4 particles cm^{-3} with the apparent formation rate of 3.1 particles $cm^{-3}s^{-1}$ during the period of 09:24 - 10:32LT. The

formation rates of two events are all within the range of typical new particle formation rates in the atmosphere (0.01-10 particles $cm^{-3}s^{-1}$, Kulmala and Kerminen, 2008).

On Day 1, a NPF event was also observed at OUC where the measurement was made during the period 09:30 to 15:13LT (Fig. 2d and e, we stopped the sampling after 15:13LT because of high relative humidity). The new particle growth curves show that the curve in the Yellow Sea after 09:30LT almost parallels to that at OUC (Fig. S2a) and the event observed at OUC advanced 1-1.5 h relative to the event observed in the Yellow Sea. Also, $N_{<30nm}$ values at the higher concentration zones, e.g., $1.6\pm0.3\times10^4$ particles cm^{-3} during 10:50 to 12:30LT in the Yellow Sea and $1.6\pm0.1\times10^4$ particles cm^{-3} during 10:50 to 13:00LT at OUC (Fig. S2b) were comparable. These suggested that NPF events occurred regionally on Day 1, but the start times were location-dependent. These higher $N_{<30nm}$ values at OUC varied in a narrow range, suggesting spatial homogeneity of nucleation in the rural area. However, these values in the Yellow Sea varied a lot. This could be due to a spatial heterogeneity of nucleation in the marine atmosphere or other unknown factors.

3.1.2 Growth rates of new particles

A two-phase new particle growth was observed in the Yellow Sea on Day 1 (Fig. 2b). 09:24-15:45LT was the first-phase growth period while the second-phase growth occurred during 17:25-18:35LT. During the first-phase growth period, the calculated $D_{pg,1}$ of new particles increased up to 39 nm with the growth rate of 5.0 nm h^{-1} (Fig. 2b, Table 1), which is close to the growth rate of 5.5 nm h^{-1} at OUC. It is interesting that no growth was observed between 15:45 and 17:25LT in the Yellow Sea but a

slight decrease of the $D_{pg,1}$ was observed from 39 nm at 16:44 to 34 nm at 17:25LT. The decrease could be explained by the shrinkage of new particles (Yao et al., 2010; Young et al., 2013). However, it also could be due to the change in measured air mass. At OUC, the $D_{pg,1}$ did not increase after 14:20LT and fluctuated at 35±1.3 nm between 14:20-15:13LT (Fig. 2e). The observations suggested that ~40 nm was likely a bottleneck for the growth of new particles in the daytime on Day 1, although the reasons remain unknown.

The $D_{pg,1}$ in the marine atmosphere restarted to increase from 34 nm at 17:25 to 47 nm at 18:35LT(after this, sampling was stopped due to high relative humidity), suggesting that the bottleneck of ~40 nm was broken up. The growth was referred as the second-phase growth. The second-phase growth rate was calculated to be 10 nm h^{-1} and the value was almost twice of the first-phase growth rate. At OUC, we did not observe the second-phase growth on Day 1 because we stopped sampling after 15:13LT. Ehn et al. (2010) reported four NPF events over the Irish west coast with the averaged growth rate of ~3 nm h^{-1}. In remote marine atmosphere, growth rates of nucleated particles were reported to be in the range of 0.1-1 nm h^{-1} (Kulmala and Kerminen, 2008, O'Dowd et al., 2010). The obviously larger growth rates observed in this event than other studies could be related to continental outflow of air pollutants which will be discussed later.

When the volume concentration of particles is considered, the amount of chemical species required for the new particle growth during the second-phase growth period (17:25 - 18:35LT) was almost same as that during the entire first-phase growth period

(09:24 - 15:45LT). This indicated that much stronger gas-particle condensation processes occurred after 17:25LT (second-phase growth), when the solar radiation substantially decreased down to a low value. Photochemical reactions were expected to be very weak at that period and cannot explain the sudden and strong condensation during the second phase growth. Alternatively, it was more likely associated with processes by thermodynamic equilibriums, e.g., when the product of nitric acid (HNO_3) and ammonia (NH_3) gaseous concentrations were higher than the thermodynamic equilibrium constant of NH_4NO_3, formation of NH_4NO_3 can suddenly take place. Formation of NH_4NO_3 often occurs in the evening or night because of decreasing ambient temperature and increasing relative humidity.

3.2 Strong NPF events in the fall cruise campaign of 2011

Two NPF events were also observed on 17 October 2011 (Day 2) in the marine atmosphere. A strong short-term NPF event was observed between 10:00-10:30LT and the estimated formation rate was 15.2 particles cm^{-3} s^{-1} (Fig. 3a and b). No subsequent growth of new particles was observed during the short-term event. A longer NPF event was observed from 10:30 on Day 2 to 03:50LT on 18 October 2011 (Day 3) when the ship sailed from H01 towards W01 (Fig. 1a). The ship was ~30 km from the coastline of Shandong peninsula in China when the longer event started to be observed. The estimated formation rate in this longer NPF event was 4.1 particles cm^{-3} s^{-1} during the period 10:30 to 11:35LT. The new particle growth rate was 2.5 nm h^{-1} during the period 10:30 to 21:40LT on Day 2 (the first-phase growth). From 21:40

on Day 2 to 02:00LT on Day 3, no particle growth was observed and the $D_{pg,1}$ fluctuated at 42±2 nm, which was similar to the particle growth bottleneck on Day 1. The second-phase particle growth occurred during the period 02:00 to 03:50LT on Day 3 when the $D_{pg,1}$ increased from 42 nm to 55 nm with the growth rate of 7.5 nm h^{-1}. Again, strong gas-particle condensation processes likely occurred after 02:00LT on Day 3 and broke up the bottleneck of ~40 nm.

Only one NPF event was observed during the period 10:15-18:20LT on Day 3 when the ship was situated at ~80 km away from the nearest coastline of Shandong peninsula and sailed westbound towards A01 station in the Yellow Sea (Fig. 1a, Fig.4a and b). However, hundreds of spikes associated with ship emissions occurred in the initial 1 h of the NPF event. When the signal of ship plumes was deducted (Fig. S3a and b, see supporting information for the approach), the estimated formation rate of new particles was 7.5 particles cm^{-3} s^{-1}. The growth rate was estimated to be 3.5 nm h^{-1} during the period 10:20 to 13:30LT and decreased down to 1.2 nm h^{-1} between 13:30 and 18:20LT. However, the maximum $D_{pg,1}$ was less than 30 nm before the signal of new particles disappeared (Table 1). The maximum value was substantially lower than the size required to activate as CCN (Dusek et al., 2006; Petters and Kreidenweis, 2007; Quinn et al., 2008; Pierce and Adams, 2009).

3.3 Weak NPF events in the fall cruise campaign of 2011

Two weak NPF events were observed on 19 October 2011(Day 4, Fig. 5a and b). A short-term NPF event started from 10:00 to 11:13LT with the formation rate of 0.3

289 particles cm^{-3} s^{-1} (Table 1). No obvious growth of new particles was observed.
290 Similarly to Day 1 and Day 2, a longer NPF event was observed during 11:13 -
291 18:30LT when the ship anchored at A02 station (Fig. 1a). The station was ~120 km
292 away from the nearest coastline. The estimated formation rate was 1.1 particles cm^{-3}
293 s^{-1}. The rate was lower than the rates observed on Day 1-3. After 11:13LT, the growth
294 rate of new particles was estimated to be 3.4 nm h^{-1}. Again, the maximum $D_{pg,1}$ was
295 less than 30 nm (Table 1). Noted that a few periodic spikes of <10 nm particles
296 constantly occurred in every 1 h and 40 min on that day, which were due to the
297 sampling artifact. Based on two-week side-by-side comparison between two identical
298 FMPS in our previous studies (unpublished), we found that the sampling artifact was
299 associated with high relative humidity, but it had negligible influence on the
300 measurement of >10 nm particles.
301 Only one NPF event was observed during the period 10:30 to 15:30LT on 26 October
302 2011 (Day 5, Fig. 6a and b) when the ship sailed from A10 towards A12. The location
303 was ~110 km away from Cheju Island of the South Korea (Fig. 1a). The estimated
304 formation rate was 1.6 particles cm^{-3} s^{-1} and the growth rate was 4.4 nm h^{-1} in the
305 initial 3 h. The $D_{pg,1}$ arrived at the maximum value of 21 nm at 13:30LT and then
306 apparently shrank down to 17 nm with a shrinkage rate of 3.5 nm h^{-1}. The shrinkage
307 of new particles has been reported in coastal environments in daytime when
308 photochemical reactions started to weaken (Yao et al., 2010; Young et al., 2013). This
309 phenomenon could also be related to slight changes of measured air mass, but the
310 influence should be minor. Since the time resolution of FMPS was as high as 1 s,

311 rapid responses of $D_{pg,1}$ and $N_{<30nm}$ corresponding to slight changes of air mass can be
312 detected, e.g., $D_{pg,1}$ and $N_{<30nm}$ fluctuated dramatically during 14:00-17:00LT on 18
313 October 2011 (Fig. 4). However, the $D_{pg,1}$ and $N_{<30nm}$ after 13:30LT on Day 5
314 decreased smoothly for one and half hours. It is interesting that preexisting particles
315 started to grow after 12:50LT, with the $D_{pg,2}$ increased from 58 nm at 12:50 to 83 nm
316 at 14:20LT, and then fluctuated at 80 ±2 nm (Fig. S4). The on-site recorded relative
317 humidity varied from 62% at 11:40 to 65% at 14:40LT and hygroscopic growth of
318 particles cannot explain the growth factor of 1.3.

319 **4. Discussion**

320 ***4.1 Cause analysis of new particle formation***

321 On Day 1, the apparent formation rate of new particles is 1.4 particles cm^{-3} s^{-1} of the
322 first short event, while the rate increase up to 3.1 particles cm^{-3} s^{-1} in the second event.
323 The ship was anchored at ~ 60 km distance from the coastline. Under the strong
324 westerly wind (10-14 m s^{-1}), it took approximately 1-2 h for air pollutants to be
325 transported from the continent to the sea zone. Moreover, the growth curve of new
326 particles in the Yellow sea after 09:30LT almost paralleled to the growth curve at
327 OUC, except for 1-1.5 h delay (Fig. S2a). Thus, we postulated that the NPF event
328 observed in the Yellow Sea after 09:24LT was probably associated with air pollutants
329 being transported from the continent. The modeling results in the sea zone, where the
330 NPF event was observed, also showed that the continental outflow of air pollutants
331 led to a slight increase of NH_4^+ and NO_3^- in concentrations after 08:00LT (Fig. 2c, Fig.
332 S5a). The modeling results apparently supported our postulation. However, we cannot

exclude other possibilities because we have no measurement for those gaseous precursors of new particles.

The weaker NPF event between 07:50-08:43LT might be associated with air pollutants being transported from the continent. However, it could also be related to ocean-derived biogenic precursors. The short duration suggested that it occurred only in the marine atmosphere. Moreover, the high wind speed would enhance air/sea exchange of gases and might increase ocean-derived biogenic precursors of new particles in concentrations, theoretically.

On Day 5, the NPF event occurred ~110 km away from the coastline of South Korea. Considering that the location of this event is far away from the polluted atmosphere, it can be speculated that it might be associated with ocean-derived gases. However, the satellite data showed that the concentration of chlorophyll a was less than 0.2 mg m^{-3} in the sea zone (Fig. S6), which was much lower than the chlorophyll a concentration (2-3 mg m^{-3}, Tan et al., 2011) in the presence of biogenic bloom in the East China Sea. Under that much low chlorophyll a condition on Day 5, ocean-derived biogenic precursors were unlikely important to this NPF event and other precursors were probably more important. The modeling results in the corresponding sea zone showed a slightly increase of SO_4^{2-} and NH_4^+ in concentrations after 10:00LT (Fig. 6, Fig. S5e). The CMAQ indeed includes sea salt emissions but there is no marine-derived gaseous sulfur, nitrogen, and carbon containing compounds. Thus, the NPF event was also possibly associated with the photochemical reactions of air pollutants being transported from the continent. Unlike on Day 5, NPF events on Day 2 were observed

355 in the coastal sea (with ~30 km from the coastline). It is well known that chlorophyll a
356 data suffer from a large interference of suspended matters in coastal seawater which
357 could not allow correctly justifying the potential influence of ocean biogenic
358 precursors on this event (Chen et al., 2013). However, higher formation rates of new
359 particles, e.g., 15.2 particles cm^{-3} s^{-1} between 10:00-10:30LT and 4.1 particles cm^{-3} s^{-1}
360 after 10:30 were observed on Day 2. The modeling results in the sea zone, where the
361 NPF event was observed, showed that the continental outflow of air pollutants led to a
362 simultaneous increase of SOA, NH_4^+ and NO_3^- in concentration after 10:00LT (Fig. 3c,
363 Fig. S5b and S7b). Thus, photochemical reactions of air pollutants from the continent
364 possibly caused the NPF event on Day 2 after 10:00LT.
365 We combined all observational data and modeling results to interpret NPF events on
366 Day 3 and Day 4. The combining results still cannot allow identifying whether air
367 pollutants transported from the continent or ocean-derived biogenic precursors caused
368 those NPF events.
369
370 ***4.2 Cause analysis of new particle growth***
371 Organics, ammonium sulfate and ammonium nitrate consisted of major parts of
372 atmospheric particles in submicron size (O'Dowd and Leeuw, 2007; Smith et al.,
373 2008; R. Zhang et al., 2009; Paasonen et al., 2010; Yao and Zhang, 2011; Ahlm et al.,
374 2012). Ambient sulfuric acid gas (H_2SO_4) has been reported to yield a negligible
375 contribution to condensational growth of >10 nm new particles (e.g., 2% of the GR of
376 7-20nm particles, Riipinen et al., 2011; Ahlm et al., 2012; Pierce et al., 2012). This

could be also true in the marine atmosphere of the marginal seas of China where the modeling mixing ratios of H_2SO_4 were less than 2 ppt during all NPF events (Figures not shown). Organics were proposed to be important contributors to grow new particles to CCN (Riipinen et al., 2011; Pierce et al., 2012). On Day 3, 4 and 5, the modeling results showed that SOA (see supporting information for detailed information of SOA modeling) was formed during the NPF events, suggesting that SOA could be an important contributor to grow new particles. The modeling results also showed that no NH_4NO_3 was formed during the entire new particle growth period on the three days in the marine atmosphere.

In addition, the temporal trend of the modeled SOA on Day 5 appeared to fit the new particle growth and subsequent shrinkage curve very well. The shrinkage of new particles occurred with a decrease of SOA in mass concentration (Fig. 6c and Fig. S7e), but the preexisting particles (> 50 nm) still grew at that period (Fig. S4).The coexistence of the shrinkage of new particles and the growth of particles (> 50 nm) were never reported in literature. Riipinen et al (2011) and Ehn et al (2014) recently reported that SOA condensation was a combination of kinetic condensation and thermodynamically partitioning of vapors on aerosol surface area. Kinetic condensation cannot explain the shrinkage from 21 nm to 17 nm. The possible explanation for the coexistence phenomenon was that the shrinkage of new particles was likely due to the Kelvin effect (Zhang et al., 2012); while particles (> 50 nm) were less affected by the Kelvin effect and they can grow to CCN size by condensation of species with relatively moderate or high volatility. However, more

399 studies are needed to examine whether the coexistence phenomenon frequently occurs
400 in polluted marine atmosphere and what caused it.
401
402 Unlike Day 3, 4 and 5, the two-phase growth of new particles was observed on Day 1
403 and Day 2. The second-phase growth occurred after a period of stagnation which was
404 regarded as a bottleneck. The modeling results on Day 1 and Day 2 showed that SOA
405 was newly formed and the temporal variation pattern of SOA was consistent to that of
406 the two-phase growth curves of new particles, suggesting the contribution of SOA to
407 the growth of new particles. However, a significant amount of NH_4NO_3 was also
408 formed during two phase growth periods which was different from that on Day 3, 4
409 and 5. And furthermore, the temporal trend of the modeled NO_3^-, NH_4^+ in mass
410 concentration generally fit the two-phase growth curve. The formation of NH_4NO_3 on
411 Day 1 and Day 2 might be one factor to break up the growth bottleneck and led to the
412 second-phase growth. In reverse, no newly formed NH_4NO_3 on Day 3, 4 and 5 could
413 be the reason for new particles being unable to break up the growth limit of 30-40 nm.
414 The modeling results showed that formation of NH_4NO_3 indeed occurred in $PM_{0.1}$
415 (Fig. S5a and b) and $PM_{2.5}$ (Fig. 2c and 3c) on Day 1 and Day 2, however, we cannot
416 confirm whether NH_4NO_3 were formed on 30-40 nm particles due to the limitation of
417 CMAQ.

418 **5. Conclusions**

419 Eight NPF events were observed on 5 days out of 31 sampling days during two cruise
420 campaigns in the marginal seas of China. By combining the observational data and the

CMAQ modeling results, we inferred that three events were probably caused by photochemical reactions of air pollutants being transported from the continent. However, the causes for other events remain unknown.

Two types of new particles growth patterns were found in the five events, i.e. one-phase growth (18, 19, 26 October 2011) and two-phase growth (4 November 2012, 17 October 2011). The maximum diameters of new particles were in the range of 20-40 nm during the three one-phase growth events and the first-phase growth period in the two-phase growth events. In two-phase growth events, new particles grew from ~40 nm to ~50 nm in later afternoon or nighttime.

The modeling results suggested that SOA could be an important contributor to the growth of new particles in the one-phase growth events, when no NH_4NO_3 was formed and H_2SO_4 had a negligible contribution to the growth of >10 nm particles. Formation of NH_4NO_3 and SOA possibly contributed to the growth of new particles in the two-phase growth events. However, the data are still limited and there are unavoidable uncertainties associated in modeling results especially SOA.

Acknowledgement

This work is funded by the National Natural Science Foundation of China (41176099, 21190050, 41121004, 41149901), the China Postdoctoral Science Foundation (2012M511548) and the Fundamental Research Funds for the Central Universities

443 (201213008).

444 **References:**

445 Ahlm, L., Liu, S., Day, D.A., Russell, L.M., Weber, R., Gentner, D.R., Goldstein, A.H., DiGangi,
446 J.P., Henry, S.B., Keutsch, F.N., VandenBoer, T.C., Markovic, M.Z., Murphy, J.G., Ren, X.R.,
447 and Scheller, S.: Formation and growth of ultrafine particles from secondary sources in
448 Bakersfield, California, J. Geophys. Res., 117, D00V08, doi: 10.1029/2011jd017144, 2012.
449 Byun, D. and Ching, J.: Science Algorithms of the EPA Models-3 Community Multiscale Air
450 Quality (CMAQ) Modeling System, EPA Report 600/R-99/030, Washington DC, available at:
451 http://www.epa.gov/amad/Research/CMAQ/CMAQdocumentation.html (last access: 15 May
452 2013), 1999.
453 Carlton, A.G., Bhave, P.V., Napelenok, S.L., Edney, E.O., Sarwar, G., Pinder, R.W., Pouliot, G.A.
454 and Houyoux, M.: Model representation of secondary organic aerosol in CMAQ v4.7,
455 Environ. Sci. Technol., 24, 8553-8560, 2010.
456 Chang, R.Y.W., Sjostedt, S.J., Pierce, J.R., Papakyriakou, T.N., Scarratt, M.G., Michaud, S.,
457 Levasseur, M., Leaitch, W.R., and Abbatt, J.P.D.: Relating atmospheric and oceanic DMS
458 levels to particle nucleation events in the Canadian Arctic, J. Geophys. Res., 116, D00S03,
459 doi: 10.1029/2011JD015926, 2011.
460 Charlson, R.J., Lovelock, J.E., Andreae, M.O., and Warren, S.G.: Oceanic phytoplankton,
461 atmospheric sulphur, cloud albedo and climate, Nature, 326, 655-661, doi: 10.1038/326655a0,
462 1987.
463 Chen, J., Zhang, X.H., and Quan, W.T.: Retrieval chlorophyll a concentration from coastal waters:
464 three-band semi-analytical algorithms comparison and development, Opt. Express, 21,
465 9024-9042, 2013.
466 Clarke, A.D., Davis, D., Kapustin, V. N., Eisele, F., Chen, G., Paluch, I., Lenschow, D., Bandy, A.
467 R., Yhornton, D., Moore, K., Mauldin, L., Tanner, D., Litchy, M., Carroll, M. A., Collins, J.,
468 and Albercook, G.: Particle nucleation in the tropical boundary layer and its coupling to
469 marine sulfur sources, Science, 282, 89-91, 1998.
470 Covert, D. S., Wiedensoler, A., Aalto, P., Heintzenberg, J., McMurry, P. H., and Leck, C.: Aerosol
471 number size distributions from 3 to 500nm diameter in the arctic marine boundary layer
472 during summer and autumn, Tellus B, 48, 197-212, 1996.
473 Curtius, J.: Nucleation of atmospheric aerosol particles, C. R. Phys., 7, 1027-1045, 2006.
474 Dal Maso, M., Kulmala, M., Riipinen, I., Wagner, R., Hussein, T., Aalto, P. P., and Lehtinen, K. E.
475 J.: Formation and growth of fresh atmospheric aerosols: eight years of aerosol size
476 distribution data from SMEAR II, Hyytiala, Finland, Boreal Environ. Res., 10, 323-336,
477 2005.
478 Dall'Osto, M., Harrlson, R.M., Furutanl, H., Prather, K.A., Coe, H., and Allan, J.D.: Studies of
479 aerosol at a coastal site using two aerosol mass spectrometry instruments and identification of
480 biogenic particle types, Atmos. Chem. Phys. Discuss., 5, doi:10.5194/acpd-
481 5-10799-200510799 -10838, 2005.
482 Dusek, U., Frank, G.P., Hildebrandt, L., Curtius, J., Schneider, J., Walter., S., Chand, D.,
483 Drewnick, F., Hings, S., Jung, D., Borrmann, S., and Andreae, M.O.: Size matters more than
484 chemistry for cloud-nucleating ability of aerosol particles, Science, 312, 1375-1378,

485 doi:10.1126/science.1125261, 2006.
486 Ehn, M., Thornton, J.A., Kleist, E., Sipilä, M., Junninen, H., Pullinen, L., Springer, M., Rubach,
487 F., Tillmann, R., Lee, B., Lopez-Hilfiker, F., Andres, S., Acir, I.-H., Rissanen, M., Jokinen, T.,
488 Schobesberger, S., Kangasluoma, J., Kontkanen, J., Nieminen, T., Kurtén, T., Nielsen, L.B.,
489 Jørgensen, S., Kjaergaard, G.H., Canagaratna, M., Dal Maso, M., Berndt, T., Petäjä, T.,
490 Wahner, A., Kerminen, V.-M., Kulmala, M., Worsnop, D.R., Wildt, J., and Mentel, T.F.: A
491 large source of low-volatility secondary organic aerosol, Nature, 506, 476-4479, doi:10.1038/
492 nature13032, 2014.
493 Feng, J.L., Guo, Z.G., Zhang, T.R., Yao, X.H., Chan, C.K. and Fang, M.: Source and formation of
494 secondary particulate matter in $PM_{2.5}$ in Asian continental outflow, J. Geophys. Res, 117,
495 D03302, doi:10.1029/2011JD016400,2012.
496 Holmes, N.S.: A review of particle formation events and growth in the atmosphere in the various
497 environments and discussion of mechanistic implications, Atmos. Environ., 41, 2183-2201,
498 2007.
499 Intergovernmental Panel on Climate Change (IPCC), Climate Change 2007: The Physical
500 OlScience Basis, edited by: Solomon, S., Dahe, Q., Manning, M., Chen, Z., Marquis, M.,
501 Averyt, K. B.,Tignor, M., and Miller, H. L.: Cambridge Univ. Press, Cambridge, United
502 Kingdom and New York, NY, USA, 153pp, 2007.
503 Kerminen, V.-M., Paramonov, M., Anttila, T., Riipinen, I., Fountoukis, C., Korhonen, H., Asmi,
504 E., Laakso, L., Lihavainen, H., Swietlicki, E., Svenningsson, B., Asmi, A., Pandis, S.N.,
505 Kulmala, M. and Petäjä, T.: Cloud condensation nuclei production associated with
506 atmospheric nucleation: a synthesis based on existing literature and new results, Atmos.
507 Chem. Phys., 12,12037-12059, doi:10.5194/acp-12-12037-2012, 2012.
508 Kulmala, M. and Kerminen, V.-M.: On the formation and growth of atmospheric nanoparticles,
509 Atmos. Res., 90, 132-150, 2008.
510 Kulmala, M., Kontkanen, J., Junninen, H., Lehtipalo, K., Manninen, H.E., Nieminen, T., Petäjä, T.,
511 Sipilä, M., Schobesberger, S., Rantala, P., Franchin, A., Jokinen, T., Järvinen, E., Äijälä, M.,
512 Kangasluoma, J., Hakala, J., Aalto, P.P., Paasonen, P., Mikkilä, J., Vanhanen, J., Aalto, J.,
513 Hakola, H., Makkonen, U., Ruuskanen, T., Mauldin III, R.L., Duplissy, J., Vehkamäki, H.,
514 Bäck, J., Kortelainen, A., Riipinen, I., Kurtén, T., Johnston, M.V., Smith, J.N., Ehn, M.,
515 Mentel, T.F., Lehtinen, K.E.J., Laaksonen, A., Kerminen, V.-M., and Worsnop, D.R.: Direct
516 observations of atmospheric aerosol nucleation, Science, 339, 943-946, 2013.
517 Lin, P., Hu, M., Wu, Z., Niu, Y., and Zhu, T.: Marine aerosol size distributions in the springtime
518 over China adjacent seas, Atmos. Environ., 41, 6784-6796, 2007.
519 Liu, X.H., Zhang, Y., Cheng, S.H., Xing, J., Zhang, Q., Streets, D.G., Jang, C., Wang, W.X., and
520 Hao, J.M.: Understanding of regional air pollution over China using CMAQ, part I.
521 performance evaluation and seasonal variation, Atmos. Environ.,44, 3719-3727, 2010a.
522 Liu, X.H., Zhang, Y., Xing, J., Zhang, Q., Wang, K., Streets, D.G., Jang C., Wang, W.X., and Hao,
523 J.M.: Understanding of regional air pollution over China using CMAQ, part II. process
524 analysis and sensitivity of ozone and particulate matter to precursor emissions, Atmos.
525 Environ., 44, 3719-3727, 2010b.
526 Luo, X. and Yu, F.: Sensitivity of global cloud condensation nuclei concentrations to primary
527 sulfate emission parameterizations, Atmos., Chem. Phys., 11, 1949-1959,
528 doi:10.5194/acp-11-1949 -2011, 2011.

O'Dowd, C.D. and Leeuw, de G.: Marine aerosol production: a review of the current knowledge, Philos. T. R. Soc. A, 365, 1753-1774, 2007.

O'Dowd, C.D., Jimenez, J.L. Bahreini, R. Flagan R.C., Seinfeld, J.H., Pirjola, L., Kulmala, M., Jennings, S.G., and Hoffmann, T.: Marine aerosol formation from biogenic iodine emissions, Nature, 417, 632-636, 2002.

O'Dowd, C.D., Monahan, C., and Dall'Osto, M.: On the occurrence of open ocean particle production and growth events, Geophys. Res. Lett., 37, L19805, dio:10.1029/2010GL044679, 2010.

Paasonen, P., Nieminen, T., Asmi, E., Manninen, H. E., Petäjä, T., Plass-Dülmer, C., Flentje, H., Birmili, W., Wiedensohler, A., Hõrrak, U., Metzger, A., Hamed, A., Laaksonen, A., Facchini, M. C., Kerminen, V.-M., and Kulmala, M.: On the roles of sulphuric acid and low volatility organic vapours in the initial steps of atmospheric new particle formation, Atmos. Chem. Phys., 10, 11223-11242, doi:10.5194/acp-10-11223-2010, 2010.

Petters, M.D. and Kreidenweis, S.M.: A single parameter representation of hygroscopic growth and cloud condensation nucleus activity, Atmos. Chem. Phys., 7, 1961-1971, doi:10.5194/acp-7- 1961-2007, 2007.

Pierce, J.R. and Adams, P.J.: Can cosmic rays affect cloud condensation nuclei by altering new particle formation rates? J. Geophys. Res., 36, L09820, doi: 10.1029/2009GL037946, 2009.

Pierce, J.R., Leaitch, W.R., Liggio, J., Westervelt, D.M., Wainwright, C.D., Abbatt, J. P.D., Ahlm, L., Al-Basheer, W., Cziczo, D.J., Hayden, K.L., Lee, A.K.Y., Li, S.M., Russell, L.M., Sjostedt, S.J., Strawbridge, K.B., Travis, M., Vlasenko, A., Wentzell, J.J.B., Wiebe, H.A., Wong, J.P.S. and Macdonald, A.M.: Nucleation and condensational growth to CCN sizes during a sustained pristine biogenic SOA event in a forested mountain valley, Atmos. Chem. Phys., 12, 3147-3163, doi:10.5194/acp-12-3147-2012,2012.

Quinn, P.K. and Bates, T.S.: The case against climate regulation via oceanic phytoplankton sulphur emissions, Nature, 480,51-56, 2011.

Quinn, P.K., Bates, T.S., Coffman, D.J., and Covert, D.S.: Influence of particle size and chemistry on the cloud nucleating properties of aerosols, Atmos. Chem. Phys., 8, 1029-1042, doi: 10.5194/acp-8-1029-2008, 2008.

Riipinen, I., Pierce, J.R., Yli-Juuti, T., Nieminen, T., Hakkinen, S., Ehn, M., Junninen, H., Lehtipalo, K., Petaja, T., Slowik, J., Chang, R., Shantz, N. C., Abbatt, J., Leaitch, W. R., Kerminen, V.-M., Worsnop, D.R., Pandis, S.N., Donahue, N.M., and Kulmala, M.: Organic condensation: a vital link connecting aerosol formation to cloud condensation nuclei (CCN) concentrations, Atmos. Chem. Phys., 11, 3865-3878, doi:10.5194/acp-11-3865-2011, 2011.

Riipinen, I., Yli-Juuti, T., Pierce, J. R., Petäjä, T., Worsnop, D. R., Kulmala, M., and Donahue, N. M.: The contribution of organics to atmospheric nanoparticle growth, Nat. Geosci., 5, 453-458, doi:10.1038/NGEO1499, 2012.

Shi, J.H., Gao, H.W., Qi, J.H., Zhang, J. and Yao, X.H.: Sources, compositions, and distributions of water-soluble organic nitrogen in aerosols over the China Sea, J. Geophys. Res: Atmos, 115, D17303, doi:10.1029/2009JD013238, 2010.

Skamarock, W.C., Klemp, J.B., Dudhia, J., Gill, D.O., Barker, D.M., Duda M., Huang, X.Y., Wang, W. and Powers, J.G.: A description of the advanced research WRF version 3, NCAR Tech. Note, Mesoscale and Microscale Meteorology Division, National Center for Atmospheric Research, Boulder, Colorado, USA, 2008.

573 Sloane, C.S., Rood, M.J., and Rogers, C.F.: Measurements of aerosol particle size-improved
574 precision by simultaneous use of optical particle counter and nephelometer, Aerosol Sci.
575 Tech., 14,289-301, 1991.
576 Smith, S. N. and Mueller, S.F.: Modeling natural emissions in the Community Multiscale Air
577 Quality, Atmos. Chem. Phys., 10, 4931-4952, doi:10.5194/acp-10-4931-2010, 2010.
578 Smith, J.N., Dumn, M.J., VanReken, T.M., Iida, K., Stolzenburg, M.R., McMurry, P.H., and Huey,
579 L. G.: Chemical composition of atmospheric nanoparticles formed from nucleation in
580 Tecamac, Mexico: evidence for an important role for organic species in nanoparticles growth,
581 J. Geophys. Res., 35, L04808, doi:10.1029/2007GL032523, 2008.
582 Tan, S.C., Shi, G.Y., Shi, J.H., Gao, H.W., and Yao, X.H.: Correlation of Asian dust with
583 chlorophyll and primary productivity in the coastal seas of China during the period from
584 1998 to 2008, J. Geophys. Res., 116, G02029, doi: 10.1029/2010JG001456, 2011.
585 Wang, Y., Zhang, R.Y. and Saravanan, R.: Asian pollution climatically modulates mid-latitude
586 cyclones following hierarchical modelling and observational analysis, Nat. Commun., 5, doi:
587 10.1038/ncomms4098, 2014.
588 Whitby, K.T.: The physical characteristics of sulphur aerosols, Atmos. Environ., 12, 135-159,
589 1978.
590 Yang, G.P., Zhang, H.H., Su, L.P. and Zhou, L.M.: Biogenic emission of dimethylsulfide (DMS)
591 from the North Yellow Sea, China and its contribution to sulfate in aerosol during summer,
592 Atmos. Environ., 43, 2196-2203, 2009.
593 Yao, X.H. and Zhang, L.: Sulfate formation in atmospheric ultrafine particles at Canadian inland
594 and coastal rural environments, J. Geophys. Res, 116, D10202, doi: 10.1029/2010JD015315,
595 2011.
596 Yao, X.H., Lau, N.T., Fang, M., and Chan, C.K.: Real-time observation of the transformation of
597 ultrafine atmospheric particle modes, Aerosol Sci. Tech., 39, 831-841, 2005.
598 Yao, X.H., Chio, M.Y., Lau, N.T., Lau, A.P.S., Chan, C.K., and Fang, M.: Growth and shrinkage
599 of new particles in the atmosphere in Hong Kong, Aerosol Sci. Tech., 44, 639-650, 2010.
600 Young, L.-H., Lee, S.-H., Kanawade, V.P., Hsiao, T.-C., Lee, Y.L., Hwang, B.-F., Liou, Y.-J., Hsu,
601 H.-T., and Tsai, P.-J.: New particle growth and shrinkage observed in subtropical
602 environments, Atmos. Chem. Phys., 13, 547-564, doi:10.5194/acp-13-547-2013, 2013.
603 Zhang, Q., Streets, D.G., Carmichael, G.R., He, K.B., Huo, H., Kannari, A., Klimont, Z., Park, I.S.,
604 Reddy, S., Fu, J.S., Chen, D., Duan, L., Lei, Y., Wang, L.T., and Yao, Z.L.: Asian emissions
605 in 2006 for the NASA INTEX-B mission, Atmos. Chem. Phys., 9, 5131-5153,
606 doi:10.5194/acp-9-5131-2009, 2009.
607 Zhang, R., Wang, L., Khalizov, A.F., Zhao, J., Zheng, J., McGraw, R.L. and Molina, L.T.:
608 Formation of nanoparticles of blue haze enhanced by anthropogenic pollution, PANS, 106,
609 17650-17654, 2009.
610 Zhang, R., Khalizov, A., Wang, L., Hu, M. and Xu, W.: Nucleation and growth of nanoparticles in
611 the atmosphere, Chem. Rev., 112, 1957-2011, 2012.
612

Figure and table

Figure 1. Cruise track during China Sea (a: Cruise during 16 October -5 November in 2011, b: Cruise during 2-11 November in 2012. Pentacles represent the locations of particle burst events).

Figure 2. New particle formation events in marine (a-c) and coastal atmosphere on 4 November 2012 (d-e) (b, e: Variations of median diameter of particle mode ($D_{pg,\ 1}$) and number concentrations of nucleation mode particles ($N_{<30nm}$) in marine and coastal atmosphere, c: CMAQ simulation of SO_4^{2-}, NH_4^+, NO_3^- and SOA in $PM_{2.5}$ in marine atmosphere).

Figure 3. New particle formation on 17 October 2011 (b: Variations of median diameter of particle mode ($D_{pg,\ 1}$) and number concentrations of nucleation mode particles ($N_{<30nm}$), c: CMAQ simulation of SO_4^{2-}, NH_4^+, NO_3^- and SOA in $PM_{2.5}$).

Figure 4. New particle formation on 18 October 2011 (b: Variations of median diameter of particle mode ($D_{pg,\ 1}$) and number concentrations of nucleation mode particles ($N_{<30nm}$), c: CMAQ simulation of SO_4^{2-}, NH_4^+, NO_3^- and SOA in $PM_{2.5}$).

Figure 5. New particle formation on 19 October 2011 (b: Variations of median diameter of particle mode ($D_{pg,\ 1}$) and number concentrations of nucleation mode particles ($N_{<30nm}$), c: CMAQ simulation of SO_4^{2-}, NH_4^+, NO_3^- and SOA in $PM_{2.5}$).

Figure 6. New particle formation on 26 October 2011 (b: Variations of median diameter of particle mode ($D_{pg,\ 1}$) and number concentrations of nucleation mode particles ($N_{<30nm}$), c: CMAQ simulation of SO_4^{2-}, NH_4^+, NO_3^- and SOA in $PM_{2.5}$).

Table 1. Major characteristics of NPF events over marginal seas of China in the fall of 2011 and 2012.

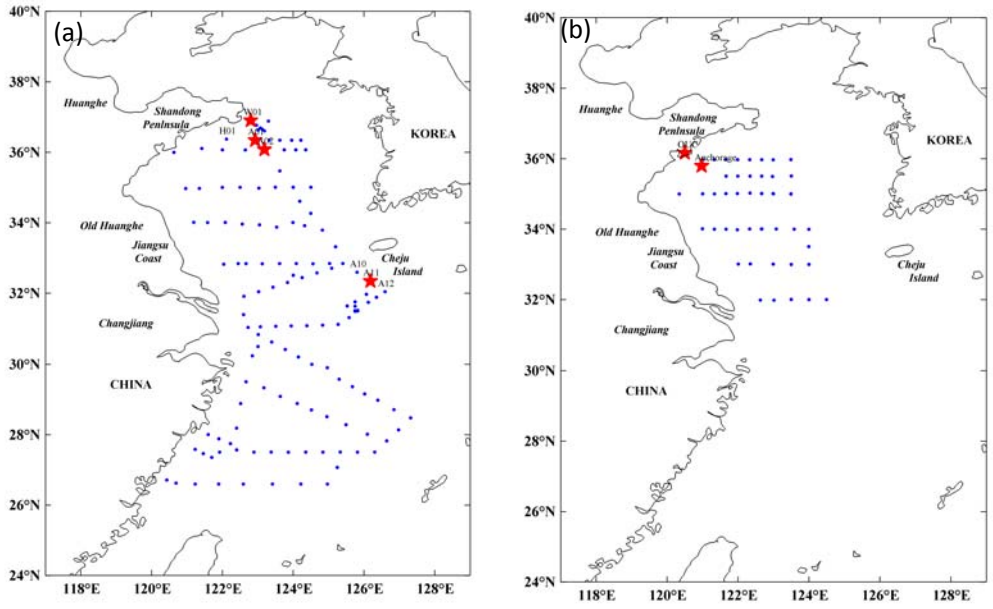

Figure 1. Cruise track during China Sea (a: Cruise during 16 October -5 November in 2011, b: Cruise during 2-11 November in 2012. Pentacles represent the locations of particle burst events).

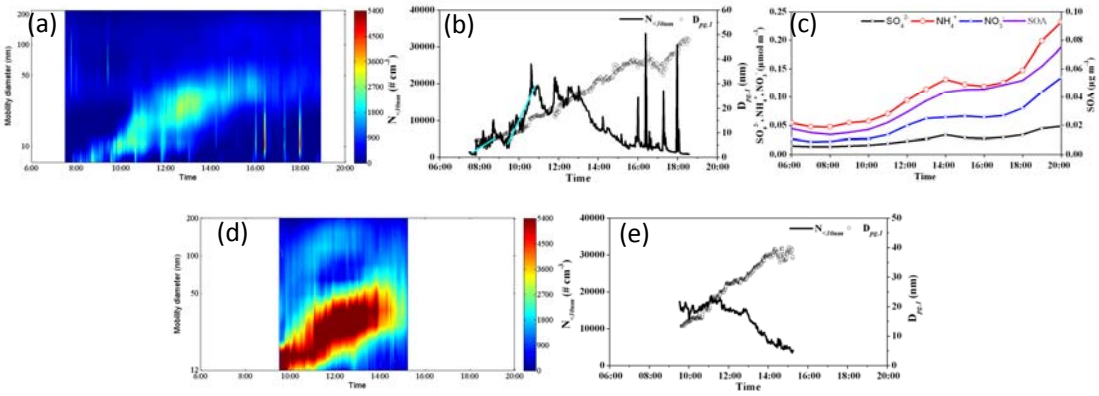

Figure 2. New particle formation events in marine (a-c) and coastal atmosphere on 4 November 2012 (d-e) (b, e: Variations of median diameter of particle mode ($D_{pg,\ 1}$) and number concentrations of nucleation mode particles ($N_{<30nm}$) in marine and coastal atmosphere, c: CMAQ simulation of SO_4^{2-}, NH_4^+, NO_3^- and SOA in $PM_{2.5}$ in marine atmosphere).

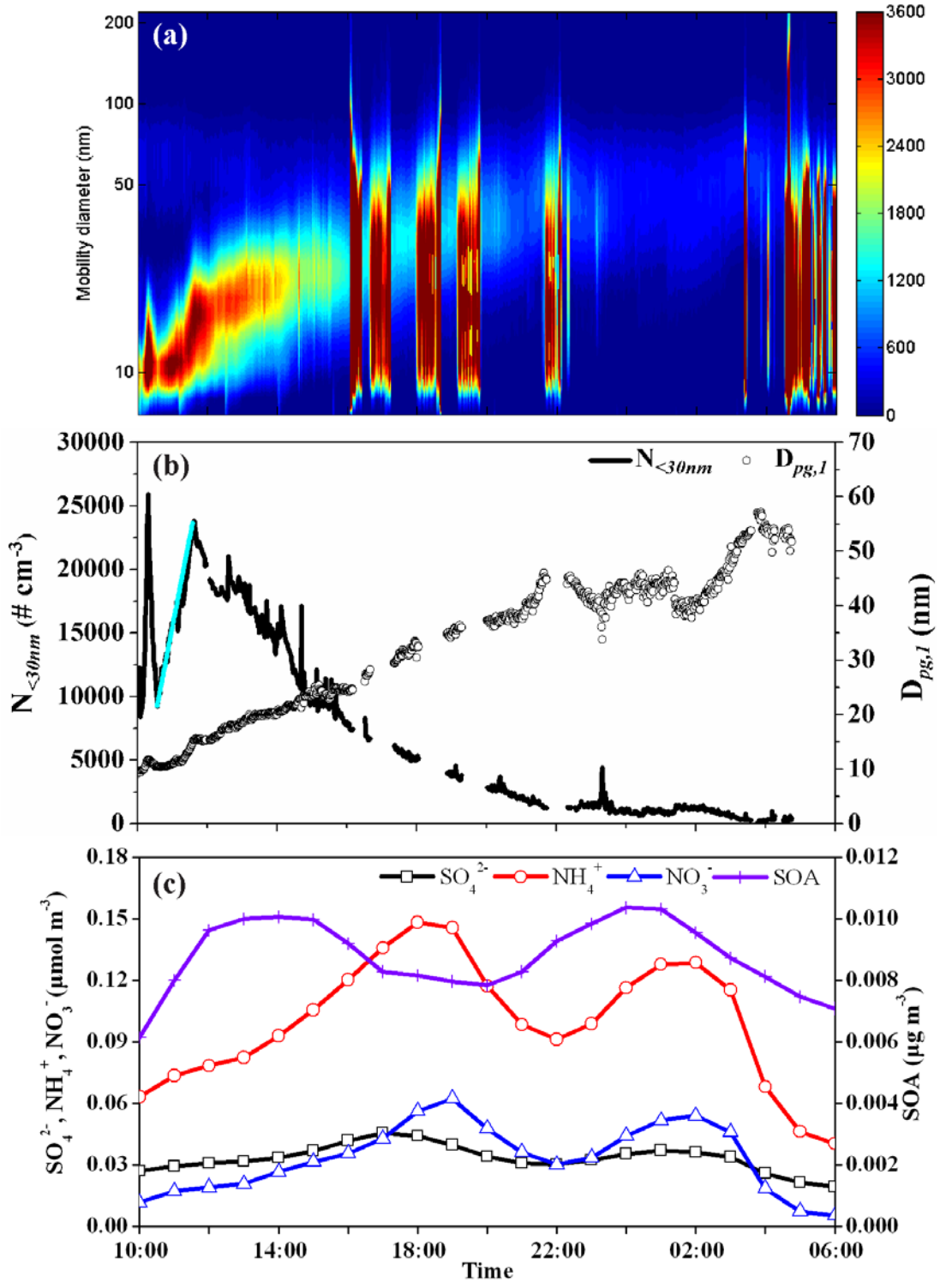

643

644 **Figure 3.** New particle formation on 17 October 2011(b: Variations of median diameter of particle

645 mode ($D_{pg,\ 1}$) and number concentrations of nucleation mode particles ($N_{<30nm}$), c: CMAQ

646 simulation of SO_4^{2-}, NH_4^+, NO_3^- and SOA in $PM_{2.5}$).

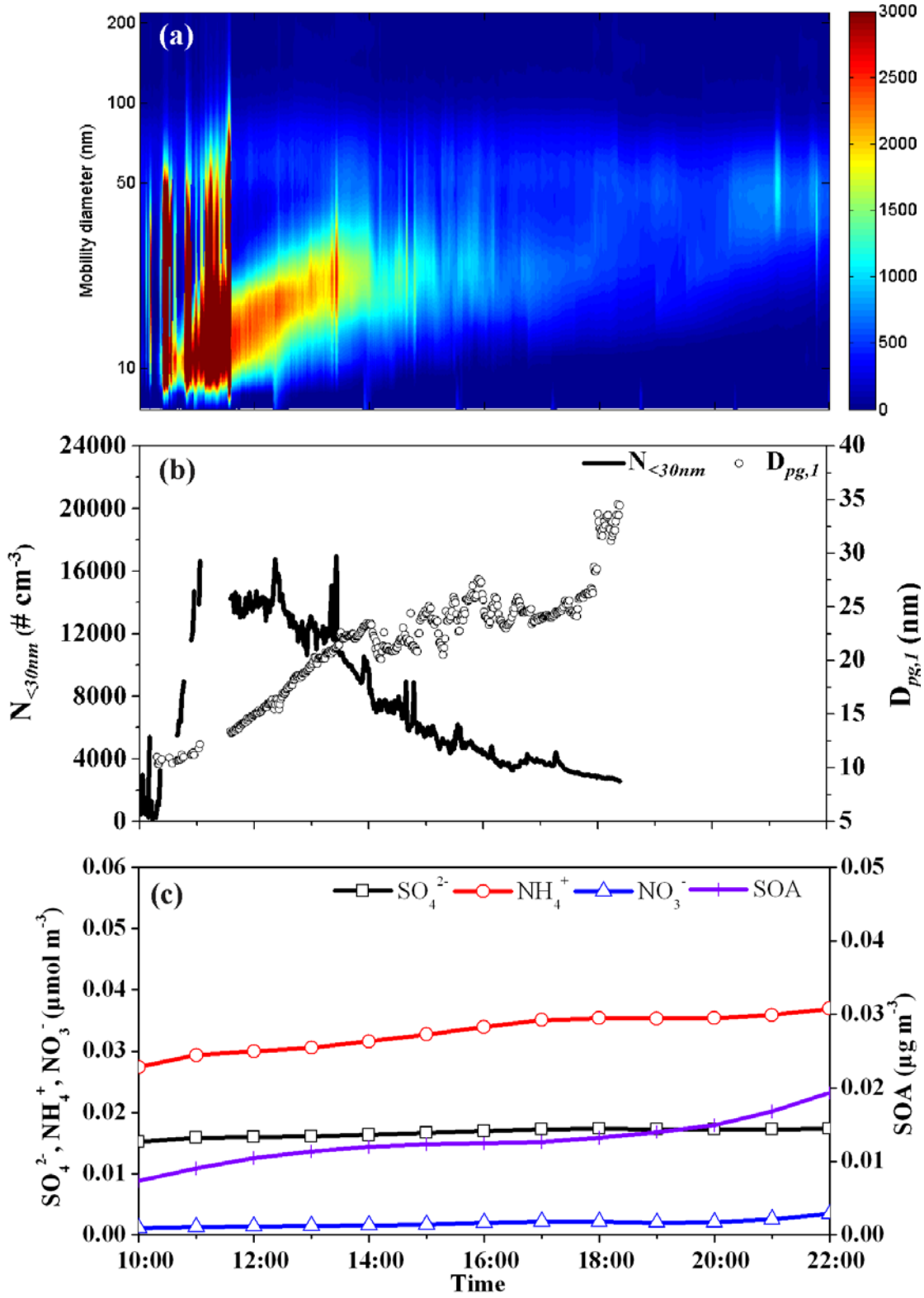

Figure 4. New particle formation on 18 October 2011. (b: Variations of median diameter of particle mode ($D_{pg,1}$) and number concentrations of nucleation mode particles ($N_{<30nm}$), c: CMAQ simulation of SO_4^{2-}, NH_4^+, NO_3^- and SOA in $PM_{2.5}$).

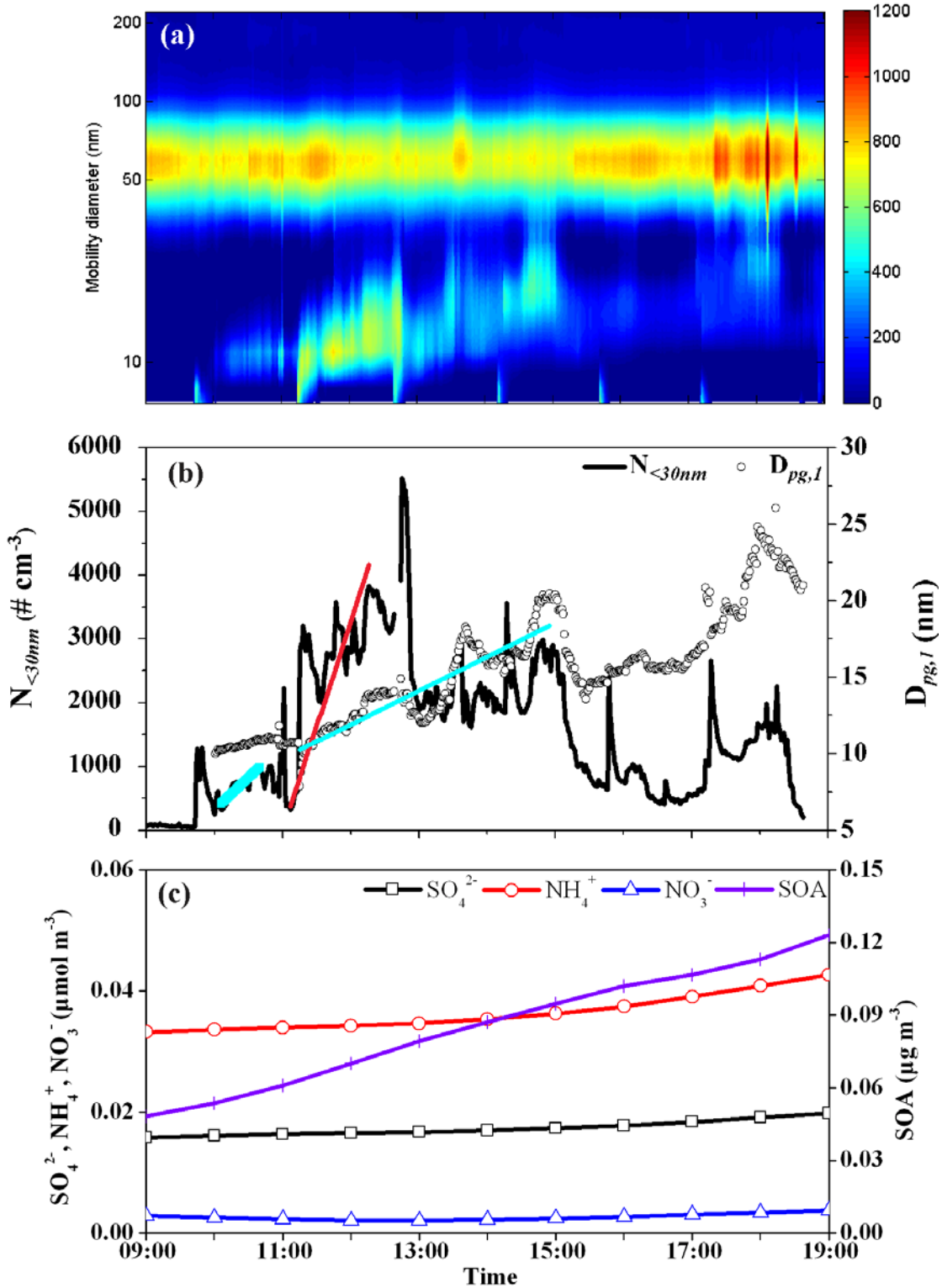

Figure 5. New particle formation on 19 October 2011 (b: Variations of median diameter of particle mode ($D_{pg,1}$) and number concentrations of nucleation mode particles ($N_{<30nm}$), c: CMAQ simulation of SO_4^{2-}, NH_4^+, NO_3^- and SOA in $PM_{2.5}$).

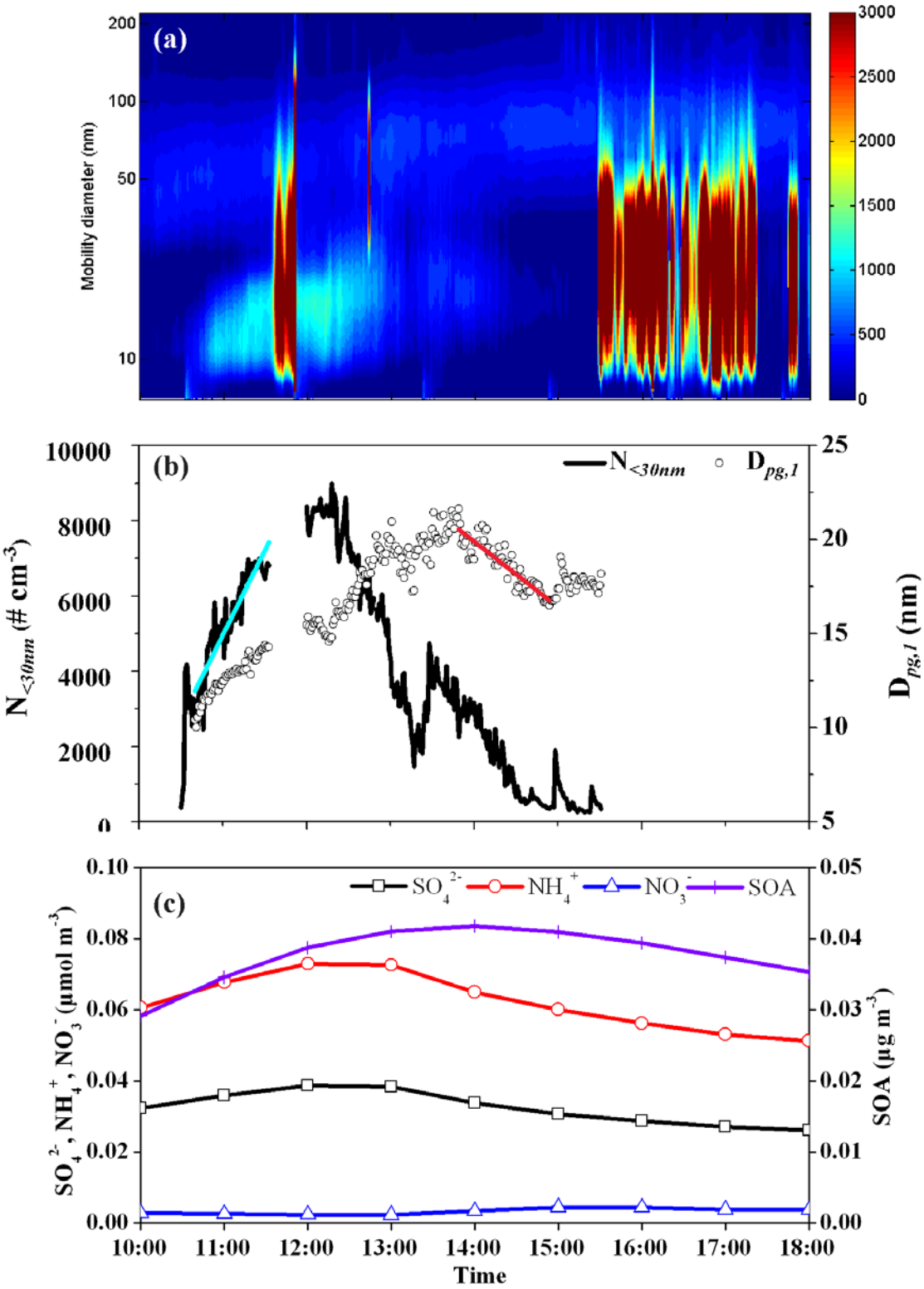

Figure 6. New particle formation on 26 October 2011 (b: Variations of median diameter of particle mode ($D_{pg,1}$) and number concentrations of nucleation mode particles ($N_{<30nm}$), c: CMAQ simulation of SO_4^{2-}, NH_4^+, NO_3^- and SOA in $PM_{2.5}$).

659 **Table 1.** Major characteristics of NPF events over marginal seas of China in the fall of 2011 and

660 2012.

Day	No.	Period	J_{30} (particles cm^{-3} s^{-1})	GR (nm h^{-1})	Location
Day 1 4 November 2012	2	7:50-8:43	1.4	-	~60 km from the land
		9:24-18:35	3.1	5.0(1^{st} stage, ~6 - 39 nm) 10.0(2^{nd} stage, 34 - 47 nm)	
Day 2 17 October 2011	2	10:00-10:30	15.2	-	H01-W01, ~30 km from the land
		10:30 (17 Oct)-03:50 (18 Oct)	4.1	2.5(1^{st} stage, 6 - 42 nm) 7.5(2^{nd} stage, 42 - 55 nm)	
Day 3 18 October 2011	1	10:15-18:20	7.5	3.5 (~6 -~28nm)	~ A01, ~80 km from the land
Day 4 19 October 2011	2	10:00-11:13	0.3	3.4 (~6 -22nm)	A02,~120 km from the land
		11:13-18:30	1.1		
Day 5 26 October 2011	1	10:30-15:30	1.6	4.4(~6 - 21nm) -3.5 (Shrinkage, 21 -17nm) 16.7 (58-83nm)*	A10-A12, ~110 km from the land

661 Note: * is the growth rate of preexisting Aitken mode particles.